# InGaAs detectors for miniature infrared instruments

T.N. Krabach, C. Staller, S. Dejewski, T. Cunningham, M. Herring, and E.R. Fossum

Jet Propulsion Laboratory, California Institute of Technology 4800
Oak Grove Drive, Pasadena, California 91109

## Abstract

In the past year, there has been substantial impetus for NASA to consider missions that are of relatively low cost as a trade off for a higher new mission launch rate. To maintain low mission cost, these missions will be of short duration and will use smaller launch vehicles (e.g., Pegasus). Consequently, very low volume, very low mass instrument (a.k.a. miniature instrument) payloads will be required. Furthermore, it is anticipated that the number of instruments flown on a particular mission will also be highly constrained; consequently increased instrument capability will also be desired. In the case of infrared instruments, focal planes typically require cooling to ensure high performance of the detectors, especially in the case of spectrometers where high D* is necessary. Since a major portion of an instrument's mass and power budget is consumed by the focal plane cooler, detector technologies that require only modest or no cooling can contribute significantly to the realization of a miniature infrared instrument. InGaAs detectors feature high D*, low dark current, and response not only in the 1 - 3 μm SWIR regime, but also in the visible regime as well. The latter feature can extend the versatility of a given spectrometer by enabling greater spectral band response while maintaining focal plane simplicity. In this paper, we discuss the InGaAs detector technology and its potential application in miniature infrared instruments.

## 1. INTRODUCTION

### 1.1 Rationale for miniature instruments

The scientific space programs of the United States, and, indeed, the entire world, are in a continuing trend toward smaller, more affordable missions. Two particular reasons toward smaller missions are 1) there has been considerable political backlash arising from the failure (or *perceived* failure) of large, expensive, and highly visible missions, such as the Hubble Space Telescope; and 2) the realities of the world economy place real limits on the resources available for the space program.

Concurrently, the scientific missions that have the highest potential for returning new knowledge are becoming increasingly challenging. In some cases, this challenge arises from the simple fact that a greater distance must be covered (e.g., a mission to Pluto); and, in other cases, the challenge arises simply from the complexity of measurements which must be made to expand the frontiers of knowledge. This latter point is typified by the emergence of the imaging spectrometer, an instrument technology in which imaging is performed simultaneously in several hundred spectral channels[1].

The combination of these trends leads to a continuing and increasing pressure to develop missions in which exciting and useful, yet limited in scope, scientific experiments can be accomplished at an affordable price. The rallying cry of "faster, better, cheaper" will likely survive for some years to come.

From the standpoint of the instrument builder, a small, affordable mission inevitably means reduced resources, such as mass, power, data rate and volume, and constraints on pointing, placement on the spacecraft, etc. These constraints have resulted in a renewed interest in technologies and techniques for reducing the size, mass, and power consumption of the various components that comprise a typical scientific instrument for space application.

### 1.2 Miniature SWIR instruments

For earth and planetary remote sensing applications, there are a broad range of scientifically important measurements to be made in the visible (0.4 - 0.7 μm, Vis), near infrared (0.7 - 1.0 μm, NIR), and short-wavelength infrared (1.0 - 2.5 μm,

SWIR). The principle reason for the importance of the wavelength regions is that they span the region of peak solar illumination. In this region, the primary phenomenology of interest is the reflectance signature of the intended target, manifested as either brightness variations, spectral reflectance variations, or both. The most commonly known subset of this group of applications is the simple electronic imaging system, of which some variant has been flown on virtually every scientific space mission. Imaging systems perform a wide variety of important measurements ranging from assessing the overall brightness, composition, and texture of the surface, to deducing atmospheric density and composition. Addition of multiple spectral filters has increased the information returned by these systems. The sophistication of traditional imaging systems has evolved along a variety of routes: 1) increased spatial resolution (of particular interest to the intelligence community); 2) broader wavelength coverage, particularly in the infrared; and 3) incorporation of traditional laboratory spectroscopy techniques in which materials are identified through their unique spectral signatures. This latter trend has led to the emergence of the imaging spectrometry concept described earlier. The SWIR provides a particularly fertile region for new and important scientific measurements: there is substantial natural illumination available from the sun; there are a broad variety of materials with unique spectral signatures in this region; and there are a variety of mature detector technologies available. Many different instruments are in operation or under construction for both earth and planetary remote sensing applications[2,3]

Miniaturization of instruments operating in the SWIR is important as an enabling technology for a wide variety of applications. For planetary exploration, for example, mission concepts are under development for a fast flyby of Pluto using a small spacecraft. Additionally, the characterization of the Mars environment through the use of an array of small sensors dropped to the surface is being developed. For Earth remote sensing, miniature instruments will be important for field measurements, operation on light aircraft, and a variety of other applications.

### 1.3 The cooling problem

Instruments operating in the infrared, including the SWIR, typically require some amount of cooling of either the detector, optics, or both. In the case of the detector, the necessity for cooling arises from the fundamental device physics in which the leakage rate is proportional to cutoff wavelength, $\lambda_{co}$. For the optics and structure, cooling is required to reduce the signal emitted, also referred to as "instrument background." This emitted energy is present at all wavelengths, but it is only in the infrared that it typically becomes an appreciable fraction of the total energy collected by the instrument.

For the SWIR, instrument background is very often not significant, and many instruments are built with moderate or no cooling of the optics or structure, leaving the detector cooling as the principal resource driver in the design of the instrument. For typical applications up to 2.5 μm, an operating temperature of 50 - 200 K may be required. Four primary technologies are in common usage for detector cooling. These technologies and their typical resource requirements are listed in the table below.

Table 1: Detector Cooling Technologies

| Technology | Temperature | Mass | Power |
|---|---|---|---|
| Radiator | > 80K | 3 - 10 Kg | none |
| Stored Cryogen | > 4K | > 50 Kg | none |
| Mechanical Cooler | > 50K | 3 - 50 Kg | 5 - 20 W |
| Thermoelectric Cooler | > 180K | < 1 Kg | 5 - 20 W |

From the table, it is apparent that there is no approach to cooling an IR detector for a SWIR application that does not require significant mass, power, or both. Many missions are visualized which would allocate only a few watts and kilograms for the entire instrument package, thus effectively precluding the use of an instrument using the current, most commonly used detector technologies.

## 2. CURRENT COOLING PENALTIES

Spacecraft infrared imagers and spectrometers requiring coolers can either choose an active or passive system; the correct cooling method to be implemented depends on the mission. All cooling systems have disadvantages, making higher operating temperature detectors very favorable. An obvious penalty of all coolers is that there is an associated mass and volume, two constrained allocations on miniature spacecraft. The Cassini mission to Saturn in 1997 will carry an infrared mapping spectrometer[3] using a passive, radiative cooler with a 0.3 $m^3$ volume and ~3 Kg mass. Several other instruments on the Cassini spacecraft also require passive coolers.

Cooler mass and volume also affect an instrument's packaging complexity. The cooler should be located near the detector for maximum cooling efficiency, thus impacting an instrument's design and placement on the spacecraft. Eliminating the cooler from an instrument will simplify the packaging complexity, and will also reduce expenses associated with instrument integration and test.

A spacecraft-related issue is the power requirements for active coolers. A solar powered spacecraft requires larger solar panels to provide the extra power necessary to operate the cooler and other aspects of the instrument. For many missions a target may be in view only once, so many instruments will collect data simultaneously increasing the power demand. Solar panels account for the vehicle's mass and are limited in the total power available for phases of a mission. Spacecraft using other sources for power (e.g., radioactive thermoelectric generators) have a limited lifetime that must be shared among all instruments. The spacecraft and mission limitations of solar power also apply to these alternative power systems.

Coolers, especially passive coolers, place extra demands on mission operations. Target imaging must consider the relative locations of the radiator, the sun, nearby warm bodies, (e.g., satellites and planets) and the target itself to maintain the detector temperature. Cost-effective missions will need to have simplified post-launch operations which higher operating temperature detectors can help achieve by reducing spacecraft maneuvers.

There are subtle impacts associated with coolers, such as contamination, vibration, reliability and lifetime. Long-term reliability has been an issue for coolers, especially mechanical coolers. To date, only passive radiators have demonstrated the reliability needed for long missions. Similarly, the cooler lifetime is a limiting factor for mission operations. A carried cryogen is limited by the amount of coolant the miniature spacecraft can carry, and a passive radiator is subject to contamination that can be seen as a gradual decrease in performance. Mechanical cooling systems have not demonstrated repeated lifetimes in excess of 2000 hours. Clearly, the elimination of the cooler will enhance the instrument's reliability and lifetime.

## 3. HIGH TEMPERATURE InGaAs DETECTORS

### 3.1 Case for higher temperature detectors

The advantages of an infrared detector that will operate at substantially higher temperatures is clear from the preceding discussion. Elimination or reduction of cooling requirements is a key ingredient in the design and construction of scientific instruments that will preserve the science capability but vastly reduce their size, mass, and cost. Two important temperature milestones for instrument design: ambient temperature, with no cooling required at all; and ~ 200K, the temperature obtainable with current state-of-the-art thermoelectric coolers (TEC). Due to the TEC's extremely small size, ruggedness, and reliability (no mechanical parts or contamination issues), it is a good choice for volume-constrained instruments. A recent design in which TEC's were the only acceptable solution is the imaging spectrometer proposed for the Lunar Scout mission. An instrument design freed from current passive or active coolers by high temperature IR arrays, can be configured into an extremely small, lightweight package.

In infrared instruments covering the SWIR region, cooling is necessary only to reduce the dark current of the detector. The background photon signal from the warm instrument is almost negligible, except perhaps at the longest wavelengths; no cooling of the optical system is needed. In such a low background environment, the focal plane sensitivity is ultimately determined by the $R_0A$ product of the photodiode. The most commonly used detector technologies in this region are indium antimonide (InSb) and mercury cadmium telluride (MCT) photovoltaic detectors. InSb requires cooling down to less than

80K, due to its small bandgap ($\lambda_{co}$ = 5.3 μm); care must be taken to ensure that background at wavelengths longer than 2.5 μm is filtered out. For MCT, the alloy concentration can be fixed to provide a bandgap equal to the longest wavelength to be observed ($Hg_{0.5}Cd_{0.5}Te$ @ 2.5 μm). The larger bandgap allows higher temperature operation; MCT arrays operating at ~150K have met BLIP limits[4] at backgrounds as low as $10^{11}$ phot/sec/cm$^2$. There are continued efforts to increase the operating temperature of SWIR MCT detectors.

Infrared detectors based on InGaAs alloys offer a solution to the contradictory demands of high sensitivity and high operating temperature. Along with higher temperature operation come further possible benefits: visible response and monolithic arrays. InGaAs is a III-V alloy whose cutoff wavelength can be varied from 0.8 μm (GaAs) to 3.5 μm (InAs). This material has not received much attention to date for scientific focal planes, primarily since it cannot respond in the 3 - 5 μm or 8 - 12 μm atmospheric windows as MCT can. However, it is a much easier material system in many respects than MCT, which translates into potentially higher figures of merit. InGaAs detectors that have been fabricated and tested already show large advantages over corresponding MCT detectors. A typical InGaAs photodetector structure is shown in Figure 1.

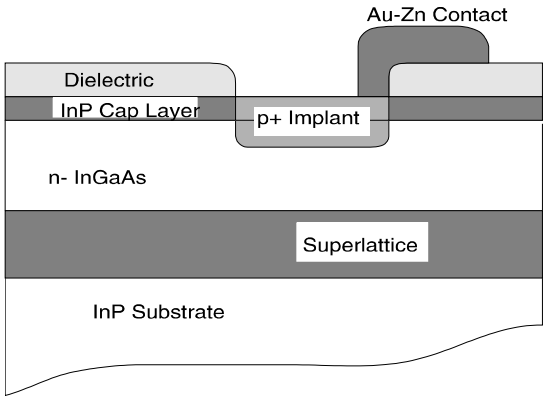


Figure 1: Structure of a simple InGaAs Photodetector

Figure 2 is a plot of $R_0A$ versus cutoff wavelength, comparing InGaAs detectors to MCT detectors with equivalent bandgaps and operating temperatures.[4,5,6,7] The advantage of InGaAs over MCT is one to two orders of magnitude! In low background instruments this translates into a 3-10x increase in SNR. This advantage can be stated another way: for equal dark currents (equivalent detectivity) InGaAs detectors can operate at temperatures perhaps 70K warmer than MCT detectors. The increased temperature margin allows the possibility of high detectivity 1.7 μm InGaAs focal planes operating at room temperature, and 2.5 μm arrays requiring only TE coolers.

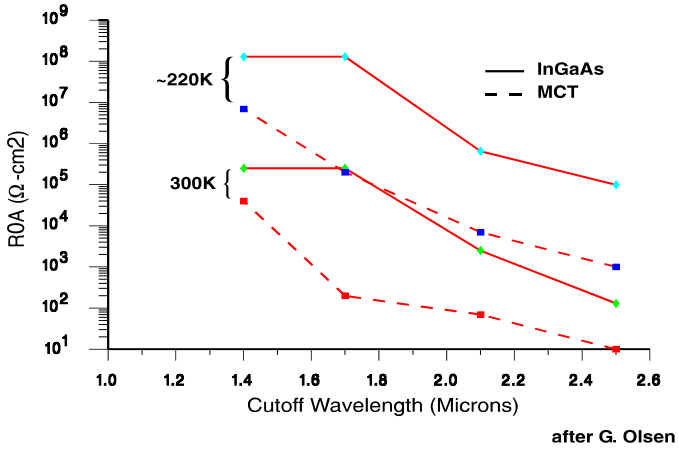


Figure 2: $R_0A$ vs cutoff wavelength for InGaAs and MCT

### 3.2 Additional advantages of InGaAs

The short wavelength response of infrared focal planes is usually limited by the substrate of the detector array in a backside illuminated design. For MCT detectors, the CdTe substrate cuts out wavelengths shorter ~0.8 μm. Many remote sensing missions demand that both visible and infrared wavelengths be sampled. This requirement leads to multiple focal planes, complex optical systems, redundant signal chains, and post processing of the data in order to register the images. A focal plane capable of operating in both the visible and the SWIR eliminates these constraints, resulting in a much more simple and compact instrument. InGaAs detectors have been fabricated in frontside illuminated configurations that offer excellent infrared response and good visible response. Figure 3 is a spectrum of an InGaAs detector ($\lambda co$ = 1.7 μm) demonstrating good quantum efficiency down to 0.7 μm, limited only by the InP cap layer over the pixel. This cap layer is deposited epitaxially and can easily be grown thinner, or eliminated, to further enhance the visible response. Further research into different passivation layers for the InGaAs surface will lead to anti-reflection coatings in order to increase the light into the active region of the diode. The result of these advances should be a focal plane responsive from below 0.5 to 2.5 μm with high quantum efficiency: ideal for many earth remote sensing applications.

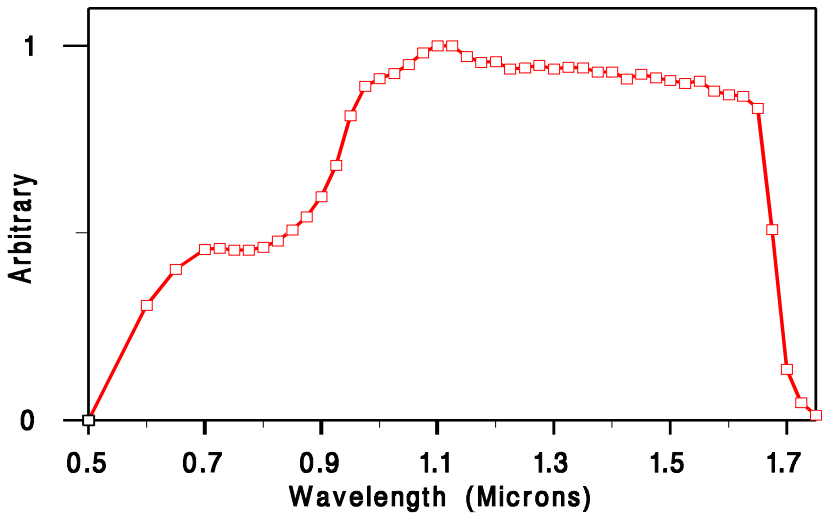


Figure 3: Normalized quantum efficiency for an InGaAs/InP lattice-matched detector

An exciting prospect in the development of InGaAs infrared sensors is the possibility of fabricating a truly monolithic SWIR focal plane with high detectivity. Integration of the readout with the photodetector has worked in silicon, but attempts at monolithic MCT arrays have met with limited success at best. Research into circuit elements based on InGaAs, however, shows that high quality components are possible. Junction field effect transistors (JFETs) and charge coupled devices (CCDs) with high performance have already been demonstrated in InGaAs. With these elements, an infrared focal plane consisting of photodiodes and an integrated readout is feasible. A monolithic FPA has several advantages over hybrid structures. The focal plane size is no longer limited by thermal matching considerations to a silicon readout chip; very large sensors, similar to that being achieved by silicon CCDs will be feasible. The indium bump bonding process is eliminated, as well as all of the processing required to mate the detector array to the readout. The cost of a monolithic sensor could be substantially less than equivalent hybrid arrays fabricated in MCT. A monolithic InGaAs focal plane will utilize front illumination; the combination will yield a single-chip focal plane with response from the visible to the SWIR.

While MCT technology for SWIR applications has benefited from the large resources applied to meet military applications at longer wavelengths, infrared focal planes based on InGaAs will be able to leverage off the enormous growth and investment of the opto-electronics integrated circuit (OEIC) industry. The demand for InGaAs diode lasers, high speed detectors, and light modulators for fiber optic communications in the 1.3 - 1.55 μm range has grown in recognition of the advantages of this material over other semiconductors. Fueled by this huge commercial interest, basic and applied material research in indium-based III-V semiconductors has grown in both university and industrial research laboratories. Development of high performance infrared detector arrays is drawing upon this research, with many results in growth techniques, transistor characterization, and InGaAs surface properties directly applicable to the fabrication of standard and unique IR sensors.

Finally, the manufacturability of InGaAs IRFPAs is potentially much greater than that of equivalent MCT hybrid arrays. Several factors lead to this potential. The first is the advanced state of growth techniques that have been developed for III-V materials. Molecular beam epitaxy (MBE), metal-organic chemical vapor deposition (MOCVD), liquid phase epitaxy (LPE), hydride-transport vapor phase epitaxy (VPE), and atomic layer epitaxy (ALE), have all been utilized. Continued research into quantum well structures incorporating indium compounds has provided a large experience base into the growth of precisely defined epitaxial InGaAs layers with controlled doping and low background impurities. The processing of InGaAs IRFPAs, as discussed above, will benefit from readily available techniques and equipment developed for the OEIC industry. A further advantage is the higher quality of III-V substrates and their more rugged nature, which can lead to yield increases over II-VI materials.

### 3.3 InGaAs growth on InP and GaAs substrates

The ternary $In_yGa_{1-y}As$ can be grown epitaxially on a III-V binary substrate. As the indium mole fraction, y, varies from $y = 0$ (pure GaAs) to $y = 1$ (pure InAs) the bandgap varies continuously from $E_g = 1.424$ eV to $E_g = 0.360$ eV, respectively[8]. The longest wavelength to which the device is sensitive, called the cut-off wavelength $\lambda_{co}$, correspondingly varies from $\lambda_{co} = 0.871$ μm to $\lambda_{co} = 3.44$ μm, respectively. At any given temperature, the device dark current increases as $E_g$ decreases because of the smaller barrier to thermal generation of electron-hole pairs. This provides the designer with a trade-off between $\lambda_{co}$ and the dark current, which the designer can optimize for a particular application by selecting the proper indium mole fraction.

There is the added complication, however, that the lattice constant of InGaAs changes as the indium mole fraction is varied. If the epitaxial InGaAs layer is not lattice-matched to the substrate, the resulting strain can generate defects and dislocations that increase the dark current by acting as generation centers. It is possible to grow strained InGaAs with a low dislocation density, but only if the InGaAs layer is thinner than a critical thickness, which is on the order of 100 Å, depending on the magnitude of the strain. Quantum-well lasers using strained InGaAs active regions have successfully been fabricated, but the allowed InGaAs layer thickness is too thin for most detector designs. The designer is therefore restricted to lattice-matched systems or strain-relaxed systems.

InGaAs with an indium mole fraction of 0.53 is lattice-matched to InP, and so can be grown strain-free on an InP substrate[910]. This fixed mole fraction limits the designer to a specific cut-off wavelength, which happens to be $\lambda_{co} = 1.7$ μm for $In_{0.53}Ga_{0.47}As$. Detectors with an $In_{0.53}Ga_{0.47}As$ active region grown on InP substrates have been made with dark current densities (at -5V) of less than 1 $\mu A/cm^2$, quantum efficiencies greater than 90%, $D^*$ values greater than $10^{12}$ cm-$Hz^{1/2}$/W, and sub nanosecond rise-times at room temperature[9]. The dark current can be reduced by more than 200 times just with thermoelectric cooling.

In order to fabricate detectors with $\lambda_{co} > 1.7$ μm, the indium mole fraction can be increased beyond 0.53, but this requires some scheme to relax the strain. One method that has been successfully used to relax the strain consists of growing a graded superlattice buffer between the substrate and the InGaAs active region[9,11-15]. This superlattice consists of layers on the order of 1 μm thickness. The lattice constant of the layer that is closest to the substrate is equal to or only slightly different from the substrate (see Figure 4). Each layer grown after that has a lattice constant closer to the InGaAs active region. Dislocations that relax the strain are generated in the thick buffer layer, but are trapped by the abrupt heterojunctions between superlattice layers, so that the dislocations do not continue into the active region, leaving it with a low defect density. Detectors with strain-relaxed InGaAs active layers with indium mole fractions up to 0.82 have been grown using the superlattice buffer technique on an InP substrate[9,11]. This technique has also been used to grow strain-relaxed InGaAs on a GaAs substrate[12-15]. At this time, the largest indium mole fraction that has been reported for strain-relaxed InGaAs on a GaAs substrate is 0.40, which is less than the 0.53 mole fraction of strain-free InGaAs on InP. Extending the indium mole fraction of InGaAs on GaAs will require the superlattice buffer to relax more strain, but effort may be worthwhile since GaAs substrates are less expensive and are usually of higher quality than InP substrates.

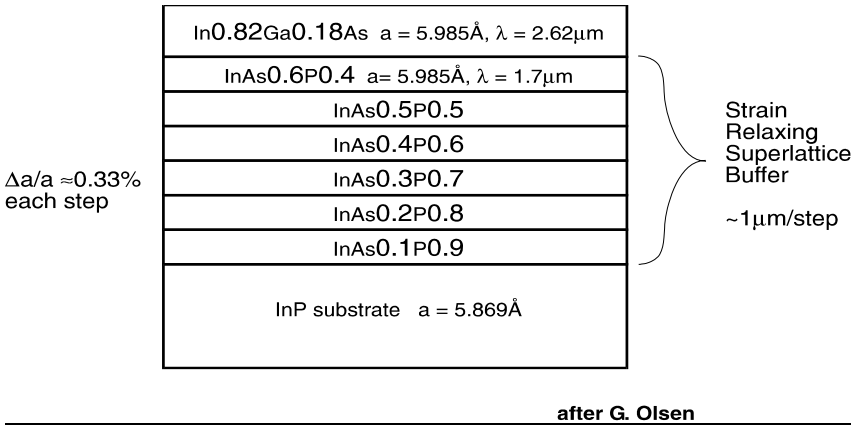


Figure 4: Use of a Superlattice buffer to relax strain at longer wavelength InGaAs on InP

Hydride VPE has been used to grow low dark current InGaAs photodiodes on InP substrates with indium mole fractions ranging from 0.53 to 0.82[11]. MBE has been used successfully to grow strain-relaxed InGaAs on GaAs substrates. Kavanagh, *et. al.,* grew $In_{0.3}Ga_{0.7}As$ on a GaAs substrate with a dislocation density of less than $2x10^5/cm^2$ and used such material to form an $In_{0.3}Ga_{0.7}As/In_{0.29}Al_{0.71}As$ heterostructure[12,13]. Such material was then successfully used to make a FET[14]. Rogers, *et. al.,*. have also fabricated strain-relaxed $In_{0.4}Ga_{0.6}As$ metal-semiconductor-metal (MSM) detectors with a cut-off wavelength of 1.3 μm on GaAs substrates[15]. These MSM detectors had a bandwidth of up to 3 GHz. Ban, *et. al.*, compared the results of lattice-matched InGaAs p-i-n detectors on InP substrates grown by hydride VPE and MOCVD. They found that both methods were capable of fabricating commercial quality devices with over 90% wafer yield[10].

## 4. CURRENT STATUS OF InGaAs DETECTORS

The development of InGaAs detector arrays for scientific applications has been enabled by the rapid advancements in InGaAs material growth and devices. These advancements have been driven primarily by the optoelectronics industry, and, to a lesser extent, the high speed transistor community. Detectors for fiber-optic communication at 1.3 μm can be ideally implemented as lattice-matched $In_{0.53}Ga_{0.47}As$/InP PIN devices. PIN detectors require high material quality to reduce dark current and decrease bit error rates. Widespread use of these devices in low-cost consumer applications drives large area wafer growth with high uniformity and reproducibility. The high intrinsic mobility of $In_{0.53}Ga_{0.47}As$ enables very high speed transistors for MMIC applications. Practical application of these transistors requires compatible growth of lattice-matched materials such as InP and $In_{0.52}Al_{0.48}As$ for the formation of insulator-like layers and channel confinement. Thus, significant knowledge has been amassed in the past decade relating to InGaAs technology. Unlike the case of HgCdTe, most of this knowledge exists in the public literature domain and is readily accessible by the scientific detector community.

Linear arrays of lattice matched $In_{0.53}Ga_{0.47}As$ have been fabricated in formats as large as 1x1024. Leakage currents of the order of 6 pA for a 25x500μm pixel size (48 $nA/cm^2$) have been reported for a 10 mV reverse bias at 300K[7]. At -5V, less than 1 $\mu A/cm^2$ dark current has been achieved. Responsivity of 0.85 A/W at 1.3 μm and 0.14 A/W at 0.8 μm has also been reported[16]. Linear arrays are typically wire bonded to a silicon multiplexer. While the $R_0A$ product of the $In_{0.53}Ga_{0.47}As$ arrays is high (e.g., $2.5x10^5$ Ω-$cm^2$ at 300 K, $1.3x10^8$ Ω-$cm^2$ at 220 K), capacitive transimpedance amplifiers are preferred over direct injection multiplexers to maximize performance in low background applications[17].

Two-dimensional arrays of 1.7 μm lattice-matched InGaAs detectors have also been reported. For example, a 128x128 $In_{0.53}Ga_{0.47}As$ array with a 60 μm pixel pitch and 40 μm x 40 μm active areas was bump-bonded to a silicon readout multiplexer. A dark current yield of greater than 99.37% (defined as pixels with dark current less than 1 nA) and a median dark current of approximately 100 pA was reported[16]. Cameras incorporating 2D arrays are under development.

Linear arrays of lattice-mismatched material have also been fabricated[17]. The growth of several layers of $InAs_yP_{1-y}$ layers between the active InGaAs layer and the InP substrate accommodates the intrinsic lattice mismatch. Increasing the indium-to-gallium ratio to increase the cutoff wavelength reduces the semiconductor energy gap and nominally results in an

increase in dark current. A mean dark current increase of a factor of 83 for 2.2 μm material and 3300 for 2.6 μm material was reported[7]. Reduction of these factors is anticipated following further development.

Lattice-matched InGaAs CCDs have also recently been reported. Two structures have been investigated. The first was a heterostructure CCD that was fabricated as an InAlAs/InGaAs/InP buried channel device[18]. The second was a two-dimensional electron gas (2DEG) InAlAs/InGaAs/InP structure[19]. Both structures exhibited significantly higher dark current than that described above for diode arrays. The transfer efficiency of the heterostructure CCD was reported as 0.98 at 13 MHz and 1 GHz. The 2DEG CCD had a higher transfer efficiency of 0.995 at 26 MHz. The relatively low transfer efficiencies and high dark currents indicate that InGaAs CCD technology is still in its infancy.

## 5. FUTURE DIRECTIONS

Clearly, the development of InGaAs technology can make a significant impact on the implementation and miniaturization of space-based Vis/NIR/SWIR instruments. For example, the near-term demonstration of a competitive 2.5 μm focal-plane array of the order of 256x256 pixels could immediately impact the design of an instrument for a fast Pluto flyby, since reduction of the radiative cooler mass could allow for alternative optimization of the instrument. A low dark current linear array with response in both the visible and the NIR/SWIR spectral regime would likely be of great interest in the design of miniature spectrometers for the exploration of Mars by miniature rovers.

The development of 2.5 μm InGaAs arrays is dependent on control of lattice-mismatch-induced defects during material growth. While, in principle, III-V growth is easier to control than II-VI ternary growth, the growth of 2.5 μm InGaAs on InP has not yet achieved the same level of maturity as lattice-matched 1.7 μm InGaAs. Continued support of 2.5 μm InGaAs material development will be required to realize its potential for scientific applications.

While lattice-matched 1.7 μm InGaAs photodiode arrays can be considered an off-the-shelf technology, they presently require hybridization to silicon multiplexers to enable focal-plane application. The present state-of-the-art of hybridized multiplexers presents two constraints on InGaAs photodiode array performance. First, the multiplexer limits the noise performance in low background applications, such as in an imaging spectrometer instrument. Input-referred read noise of silicon multiplexers is typically in the 30-50 electrons r.m.s. level range[20]; state-of-the-art scientific silicon CCDs are currently achieving 3-5 electrons r.m.s. read noise[21]. Thus, reduction of multiplexer read noise is of great interest.

A second limitation of current 2D array hybridization schemes is that bump-bonding forces the illumination of the detector array from the backside. In the case of InGaAs/InP structures, this configuration limits the short wavelength response to the absorption edge of InP (approximately 0.9 μm). Thus, the ability of the InGaAs photodiodes to respond to visible illumination is precluded by the substrate. While thinning the substrate is possible (in principle), frontside illumination of the array would be preferred. Thus, either a hybrid multiplexer that allows for frontside illumination of the detector array is required, or a monolithic detector array/multiplexer such as a CCD needs to be developed.

Recognizing the difficulties in achieving an InGaAs CCD technology, JPL has developed a new concept for the implementation of InGaAs detector arrays that allows for monolithic readout[22]. This concept, known as an *active pixel sensor*, should allow both visible response[23] and reduction in read noise of the InGaAs photodetector. The JPL active pixel sensor structure is shown below in Fig. 5. The active pixel concept incorporates both the photodetector and the output amplifier into the pixel. The structure trades readout performance for fill-factor since a portion of the pixel area is used for the output amplifier. The device is configured as a single-stage buried-channel junction CCD. Signal charge is collected under the photogate (PG). Just prior to readout, the output collector is reset using JFET R. The signal is then transferred into the low capacitance output collector. The change in voltage on this node is buffered by the source-follower and output to a column bus, as selected by JFET S. This structure, presently under investigation, is expected to yield good visible, NIR, and SWIR response since it is frontside illuminated. High sensitivity is also expected. The JFET transistors should minimize noise, and the readout timing is designed to allow both correlated double sampling (CDS) and good 1/f noise rejection. Input referred noise is anticipated to be below 10 electrons r.m.s. A 40 μm x 40 μm pixel is expected to have a fill-factor greater than 50%. A linear array configuration would have 100% fill-factor since the output amplifier can be located adjacent to the pixel beyond the active region.

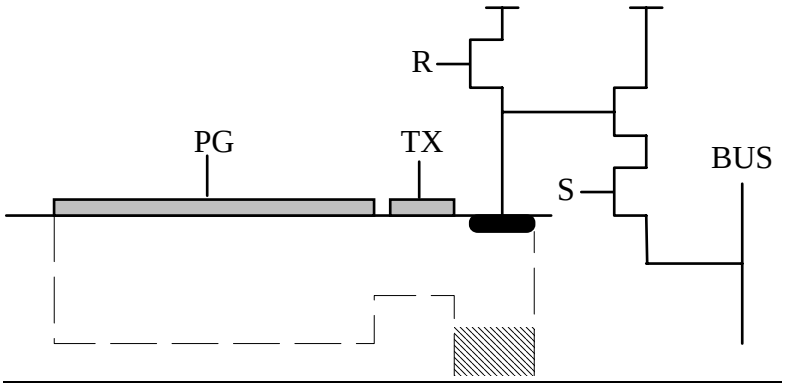


Fig. 5: JPL active pixel structure for InGaAs photodetector arrays.

## 6. ACKNOWLEDGMENTS

The authors appreciate the assistance of Dr. G. Olsen of Sensors Unlimited in gathering some of the information used in this paper. Discussions with Dr. M. Greiner of Cincinnati Electronics, Dr. P. Kirchner of IBM, Prof. H. Wieder of UCSD, and Mr. L. Kozlowski of Rockwell International are also appreciated. The support of Dr. V. Sarohia of JPL is also appreciated.

The research described in this paper was carried out by the Jet Propulsion Laboratory, California Institute of Technology, under a contract with the National Aeronautics and Space Administration.

Reference herein to any specific commercial product, process, or service by trade name, trademark, manufactureer, or otherwise, does not constitute or imply endorsement by the United States Government or the Jet Propulsion Laboratory, California Institute of Technology.

## 7. REFERENCES

[1]M. Herring, T. Chrien, V. Duval, T. Krabach, "Imaging Spectrometry - Concepts and System Tradeoffs," *Proc. SPIE Vol 1874 (in press).*

[2]M.L. Eastwood, C.M. Sarture, T.G. Chrien, R.O. Green, W.M. Porter, "Current instrument status of the airborne visible/infrared imaging spectrometer (AVIRIS)," *Proc. SPIE*, Vol. 1540, pp. 164-175 (1991).

[3]J.B. Wellman, J. Duval, D. Juergens, J. Voss, "Visible and infrared mapping spectrometer (VIMS): a facility instrument for planetary missions," *SPIE*, Vol 834, p. 213 (1987).

[4]L.J. Kozlowski, K.Vural, W.E. Tennant, R.Kezer, and W.E. Kleinhans, "Low Noise 2.5 um PACE-1 HgCdTe 10x132 FPA with 25 um Pitch and On-Chip Signal Processign Including CDS and TDI," Proceddsings of IRIS Specialty Group on Infrared Detectors Vol. II, NIST, Boulder, CO, p. 155.

[5]L.J. Kozlowski, S.L. Johnston, W.V. Mclevige, A.H.B. Vanderwyck, D.E. Cooper, S.A. Cabelli, E.R. Blazejewski, K.Vural, W.E. Tennant, "128x128 PACE-1 HgCdTe hybrid FPAs for Thermoelectrically-Cooled Applications", *Proc. SPIE* Vol. 1685 (Orlando, 1992).

[6]G.Olsen, A. Joshi, M.Lange, K. Woodruff, E. Mykietyn, D. Gay, G. Erikson , D. Ackley, V. Ban, C Staller, " A 128x128 InGaAs Detector Array for 1.0 1.7 um", *Proc. SPIE* Vol. 1314, (1990), p31.

[7]A.M. Joshi, G.H. Olsen, S. Mason, M.J. Lange, and V.S. Ban, "Near Infrared (1-3 μm) InGaAs Detectors and Arrays: Crystal Growth, Leakage Current and Reliability," *Proc. SPIE* Vol. 1715, paper 63 (1992).

[8]H.C. Casey and M.B. Panish, *Heterostructure Lasers Part B*, Academic Press, Inc., Harcourt Brace Jovanovich, Publishers, San Diego, CA (1978).

[9]G.H. Olsen, "InGaAs fills the near-IR detector-array vacuum," *Laser Focus World*, Vol 27(3), pA21 (1991).

[10]V.S. Ban, K.Woodruff, M. Lange, G.H. Olsen, and K.A. Jones, "Comparison of InGaAs/InP p-i-n detectors grown by hydride and organometallic vapor phase epitaxy," *IEEE Transactions on Electron Devices*, Vol 37(3), p814 (1990).

[11]K.R. Linga, G.H. Olsen, V.S. Ban, A.M. Joshi, and W.F. Kosonocky, "Dark current analysis and characterization on $In_xGa_{1-x}As/InAs_yP_{1-y}$ graded photodiodes with x>0.53 for response to longer wavelengths (>1.7 μm)," *IEEE Journal of Lightwave Technology*, Vol 10(8), p1050 (1992).

[12]K.L Kavanagh, J.C.P. Chang, J. Chen, J.M. Fernandez, and H.H. Weider, "Lattice tilt and dislocations in compositionally step-graded buffer layers for mismatched InGaAs/GaAs heterointerfaces," *J. Vac. Sci. Tech. B* Vol 10(4), p1820 (1992).

[13]J. Chen, J.M. Fernandez, JCP Chang, K.L. Kavanagh, and H.H. Wieder, "Modulation-doped $In_{0.3}Ga_{0.7}As/In_{0.29}Al_{0.71}/As$ heterostructures grown on GaAs by step grading," *Semicond. Sci. Tech.* Vol 7, p601 (1992).

[14]N.C. Tien, J. Chen, J.M. Fernandez, and H.H. Wieder, "Unstrained, Modulation-Doped, $In_{0.3}Ga_{0.7}As/In_{0.29}Al_{0.71}/As$ field-effect transistor grown on GaAs substrate," *IEEE Electron Device Letters*, Vol 13(12), p621 (1992).

[15]D.L. Rogers, J.M. Woodall, G.D. Pettit, and D. McInturff, "High-speed 1.3-μm GaInAs detectors fabricated on GaAs substrates," *IEEE Electron Device Letters*, Vol 9(10), p515 (1988).

[16]G.H. Olsen, "InGaAs fills the near IR detector array vacuum," *Laser Focus World*, March 1991.

[17]A.M. Joshi, V.S. Ban, S. Mason, M.J. Lange, and W.F. Kosonocky, "512 and 1024 elementl inear InGaAs detector arrays for near infrared (1 - 3❍m) environmental sensing," *Proc. SPIE*, Vol 1735 (1992).

[18]D.V. Rossi, J.-I. Song, E.R. Fossum, P.D. Kirchner, G.D. Pettit, and J.M. Woodall, "A Resistive-Gate $In_{0.53}$ $Ga_{0.47}As/InP$ Heterostructure CCD," *IEEE Electron Device Lett.*, vol. EDL-12(12) pp. 688-690 (1991).

[19]D.V. Rossi, A. Cheng, H. Wieder, and E.R. Fossum, "A Resistive-Gate InAlAs/InGaAs/InP 2DEG CCD," *Proc. 1992 IEEE International Electron Devices Meeting*, San Francisco, CA December 1992.

[20]F. Low, "Unfulfilled needs in IR astronomy focal plane readout electronics," in Infrared Readout Electronics, *Proc. SPIE*, Vol. 1684, pp. 168-174 (1992).

[21]J. Janesick and T. Elliot, "History and advancement of large area scientific CCD imagers," in Astronomical Society Pacific Conference Series, 1991, Tucson, AZ.

[22]E.R. Fossum, T.J., Cunningham, T.N. Krabach, and C.O. Staller, Active Pixel Sensor Structure Using Junction Field-Effect Devices, JPL New Technology Report, NPO 8562/18978, September 1992.

[23]S. Kagawa, K. Inoue, I. Ogawa, Y. Takada, and T. Shibata, "Wide-wavelength InGaAs/InP PIN photodiodes sensitive from 0.7 to 1.6 μm," Jap. J. Appl. Phys. Vol. 28(10) pp. 1843-1846 (1989).